The new CLOCIT irradiation facility for $^{40}Ar/^{39}Ar$ geochronology: Characterization, comparison with CLICIT, and implications for high-precision geochronology

Daniel Rutte[a,b], Tim A. Becker[a], Alan L. Deino[a], Steven R. Reese[c], Paul R. Renne[a,b], and Robert A. Schickler[c]

[a] Berkeley Geochronology Center, 2455 Ridge Road, Berkeley, CA 94709, USA

[b] Department of Earth and Planetary Science, University of California, Berkeley, CA 94720, USA

[c] Nuclear Science and Engineering, Oregon State University, Corvallis, OR 97331, USA

Abstract

The Cadmium-Lined Outer-Core Irradiation Tube (CLOCIT) is a new irradiation facility for $^{40}Ar/^{39}Ar$ geochronology at the Oregon State University TRIGA® reactor. We report fluence parameters from the first four CLOCIT irradiations and compare them to the existing Cadmium-Lined Inner-Core Irradiation Tube (CLICIT). CLOCIT provides an average neutron flux equivalent of 1.45–1.53 $\times 10^{-4}$ *J*/h; about 55% of CLICIT. Radial fluence gradients are on the order of 0.2–2.4 %/cm. A planar fit of *J*-values results in residuals in the range of uncertainty in the *J*-value, but systematic deviations resolve a non-planar component of the neutron flux field which has also been observed in CLICIT. Axial neutron fluence gradients are 0.6–1 %/cm, compared to 0.7–1.6 %/cm for the CLICIT. Production rate ratios of interfering reactions are $(^{40}Ar/^{39}Ar)_K = (4\pm6) \times 10^{-4}$ and $(^{38}Ar/^{39}Ar)_K = (1.208\pm0.002) \times 10^{-2}$, $(^{36}Ar/^{37}Ar)_{Ca} = (2.649\pm0.014) \times 10^{-4}$, $(^{38}Ar/^{37}Ar)_{Ca} = (3.33\pm0.12) \times 10^{-5}$, and $(^{39}Ar/^{37}Ar)_{Ca} = (9.1\pm0.28) \times 10^{-4}$, similar to the CLICIT values.

Introduction

The Cadmium-Lined Inner-Core Irradiation Tube (CLICIT) in the TRIGA® reactor at Oregon State University (OSU) is a highly utilized irradiation facility for $^{40}Ar/^{39}Ar$ geochronology. In 2017, 79 irradiations were conducted for 23 labs from 12 different countries. Increased CLICIT demand has led to sample backlogs of up to 300 h with OSU limited to 35 h of operation a week. Responding to demand, a second facility, the Cadmium-Lined Outer-Core Irradiation Tube (CLOCIT), has been commissioned. Here we report results from the first four irradiations spanning 17 minutes to 32.25 hours to characterize the new facility. We document average $^{39}Ar_K$ production rates, neutron fluence gradients, and production rate ratios of interference reactions on Ca and K. We compare these values to data from four recent CLICIT irradiations and production rate ratios on Ca and K established over the long term.

Technical Specifications

The CLOCIT is identical in construction to the CLICIT (Schickler et al., 2013). It consists of two aluminium tubes: the inner tube has an outer diameter (OD) of 31.75 mm with a wall thickness of 1.47 mm. Surrounding the bottom of the inner tube is an outer tube which is 37.5 mm OD with a wall thickness of 1.45 mm. This outer tube is 1067 mm long and serves as the facility's in-core terminus. To minimize thermal neutron penetration into the irradiation facility, a 0.508 mm thick Cadmium sleeve is wrapped around the outside of the inner aluminium tube and a disc of Cadmium is placed at its bottom (Schickler et al., 2013). The facility allows irradiation of cylindrical packages with an OD of 22.86 mm and a height of 101.6 mm.

An MCNP (Monte Carlo n-particle) transport model of the reactor was employed to identify a position for CLOCIT that provides a high fast-neutron flux at an acceptable loss of reactivity with the Cadmium sleeve introduced (Schickler and Reese, 2017). Position F20 near the core periphery, but still surrounded by fuel elements provides this compromise (Figure 1). Two new fuel rods were added to the core inventory and graphite rods were shuffled to minimize the loss in reactivity.

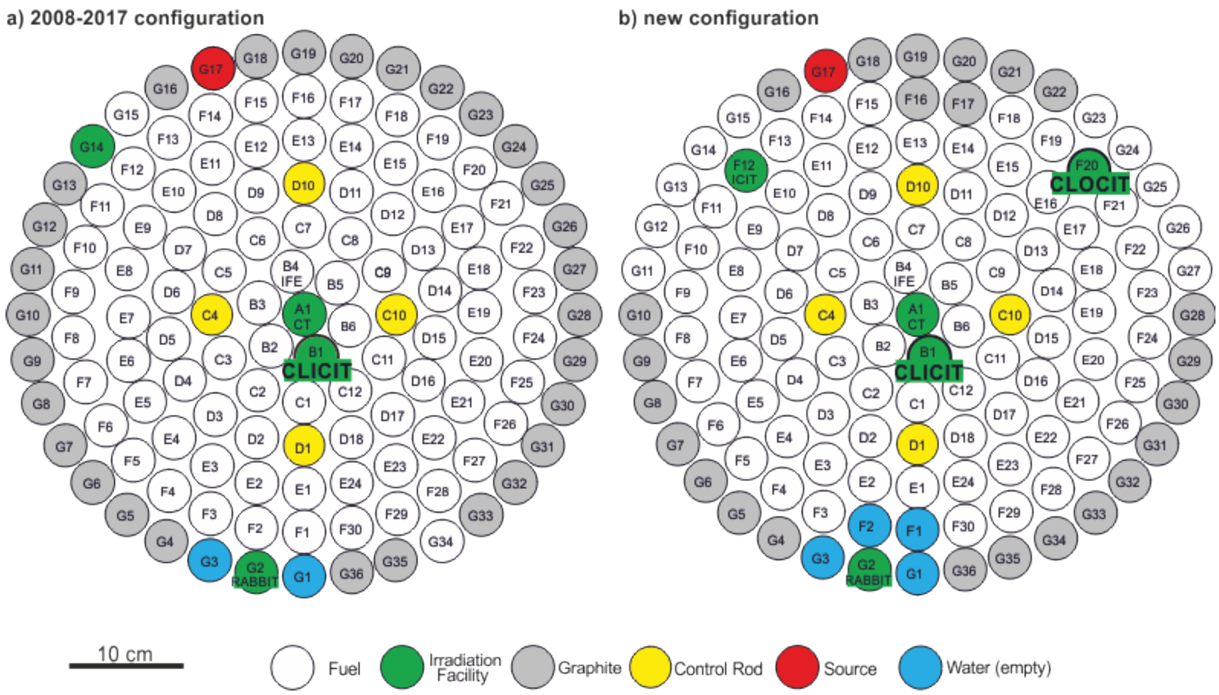

Figure 1. Diagram of the reactor core configurations a) before and b) after installation of the CLOCIT.

The axial flux profiles in the CLOCIT and CLICIT were determined by activation of 55 cm long Al-Au wire ($^{197}Au(n,\gamma)^{198}Au$) and subsequent gamma spectrometry of ^{198}Au activity. The axial flux profile is the expected bell shape (Figure 2). OSU has historically determined 20 cm above the base of the core as the desired location for irradiation of $^{40}Ar/^{39}Ar$ samples; thus a 20 cm tall installed pedestal ("saddle") ensures the samples are irradiated at the axial peak of the neutron flux. The height can be adjusted to the needs of a specific irradiation by addition of sample spacers.

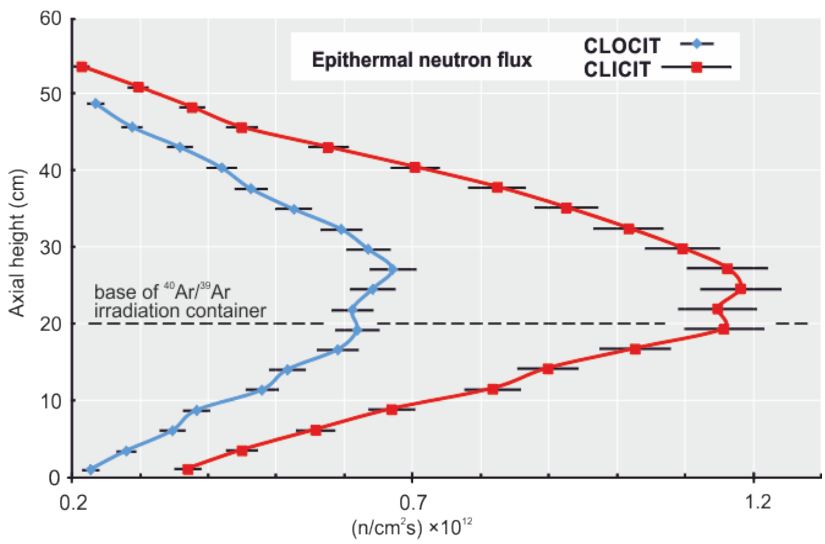

Figure 2. Axial flux profile of the CLOCIT and CLICIT determined by irradiation and subsequent γ-spectrometry of Al-Au wire.

Methodology

We determined neutron fluences by irradiation and analysis of widely used geological sanidine standards from the Fish Canyon Tuff (FCs; ~28.2 Ma) and the Alder Creek rhyolite (ACs; ~1.18 Ma), and calculation of *J*-values (Formula 1; Grasty and Mitchell, 1966). Formula 1 shows the relation of the ratio of $^{40}Ar^*$ (radiogenic ^{40}Ar) and $^{39}Ar_K$ (^{39}Ar activated from K) in a standard of known age t with the neutron fluence Φ and their abstraction as the *J*-value. ^{39}K and ^{40}K are the respective natural abundances, λ is the total decay constant of ^{40}K, λ_e its electron capture decay constant, and σ the cross section of $^{39}K(n,p)^{39}Ar$ as a function of neutron energy E. For a detailed derivation see Grasty and Mitchell (1966).

$$J = \frac{^{39}K}{^{40}K}\frac{\lambda}{\lambda_e}\int \Phi(E)\sigma(E)\,dE = \frac{e^{\lambda t}-1}{\frac{^{40}Ar^*}{^{39}Ar_K}} \qquad \text{Formula 1}$$

Grains of 0.25–0.3 mm (FCs) and 0.60-0.71 mm (ACs) were loaded in aluminium disks with a diameter of 18.54 mm (Figure 3). 4 to 6 wells outlining a square, pentagon or hexagon along the edge of the disk - spanning about 15 mm across – and in some disks additional wells in the centre of the disk were loaded with FCs or ACs. In irradiation 468 we included crushed synthetic Fe-doped glass of kalsilite composition ($KAlSiO_4$) with a grain size of 0.4–0.6 mm around the centre of level A and crushed natural fluorite with a grain size of 0.2–0.4 mm around the centre of level B. The disks were wrapped in Al foil, stacked and encapsulated in tight-fit glass tubing (preventing tilting of the disks).

We individually analyzed 5–10 grains of ACs and FCs per well, heated in one or two steps and calculated an inverse-variance weighted mean (in the following "weighted mean") *J*-value for the respective well. All three Ar analysis lines at BGC (NEXUS, Map1, and Noblesse) were involved, using measurement routines described in Niespolo et al. (2017). Typical uncertainties of *J*-values of individual wells are ~0.15–0.4%. We determined a planar fit through the 4–8 wells of given *J*-value and calculated the deviation of each well from the fitted plane; the calculation considers uncertainty in *J*-value and predicts a *J*-value and respective uncertainty for any position. For *J*-value calculations we used ages of 28.201Ma (Kuiper et al., 2008) and 1.1848 Ma (Niespolo et al., 2017)) for FCs and ACs, respectively. Other ages are in use for these standards but the values used are irrelevant for the present purposes so long as they are internally consistent as was demonstrated by Niespolo et al. (2017).

Results and Discussion

Average Neutron Flux

The average flux in the CLOCIT irradiations is equivalent to 1.45–1.53 $\times 10^{-4}$ *J*/h (Table 1). These values compare to 2.62–2.72 $\times 10^{-4}$ *J*/h of the last four CLICIT irradiations analyzed at BGC. Thus to achieve a similar *J*-value, CLOCIT irradiations should be about 1.8 times longer than those in the CLICIT.

Table 1. Comparison of fluence parameters of four irradiations in CLOCIT and CLICIT, respectively.

Irradiation	duration [h]	level	n	height in irradiation container [cm]	radial gradient [%/cm]	max. dev. from planar fit [%]	axial grad. [%/cm]	J/h $\times 10^{-4}$
CLOCIT:								
468	32.25	A	5	0.2	0.16	0.25		1.452
		B	5	2.8	0.40	0.13	1.0	1.509
		C	5	5.3	0.58	0.07		1.529
470	0.28	A	4	0.2	0.83	0.26	NA	1.513
471	0.83	A	4	1.9				
		B	4	1.3	2.4	0.35	0.4	1.466
		C	4	0.8	1.8	0.12		1.467

		D		0.2	0.0	0.15		1.459
472	5	A	4	1.9	1.8	0.01		1.474
		B	4	1.3	1.5	0.07	0.6	1.465
		C	4	0.0	1.5	0.13		1.459
		D	4	0.2	1.8	0.05		1.458
CLICIT:								
464	0.5	A	4	1.0	0.07	0.02	1.6	2.715
		B	4	0.2	0.96	0.25		2.682
465	2	A	4	1.0	0.04	0.31	1.4	2.647
		B	4	0.2	0.54	0.20		2.619
466	20	1	7	0.2	0.29	0.31		2.654
		2	7	1.1	0.23	0.32	0.7	2.664
		3	7	2.0	0.23	0.44		2.692
		4	7	2.9	0.05	0.41		2.697
467	1	A	6	2.9	0.06	0.22		2.702
		B	6	2.0	0.13	0.68	0.9	2.682
		C	6	1.1	0.21	0.14		2.650
		D	3	0.2	0.49	NA		2.642

Fluence Gradients

The axial fluence increases upwards from the basal standard irradiation position by an average of about 0.6–1 %/cm in the CLOCIT, similarly the CLICIT (0.7–1.6 %/cm; Table 1). For irradiation sample holders utilizing wells in an aluminium disk, these gradients may be significant when standards and unknowns have different fill levels in the wells.

We calculated radial gradients based on planar fit through the weighted mean *J*-values of wells. The maximum deviation of individual wells from the planar fit is typically below 0.3% for both CLICIT and CLOCIT (Table 1) and in the range of analytical uncertainty of the *J*-value indicating that planar fits provide a decent approximation on the scale of a disk. However, we found a systematic deviation of the central wells to lower *J*-values. The 7 disks with standards in the central well (both CLICIT and

CLOCIT irradiations) gave a weighted mean analyzed-over-predicted ratio of 0.9982±0.0009 (MSWD=0.73), i.e., in average 0.2% lower values. Both the larger distance of the central well to the surrounding fuel elements and neutron shielding by the irradiation container and samples may contribute to this. Rutte et al. (2015) provides a simulated neutron flux distribution that illustrates the significantly non-planar axial variation over the irradiation channel in a comparable research reactor without an irradiation target introduced (their figure 4b). Shielding includes consumption of neutrons by capture and transfer reactions as well as neutron moderation by scattering; moderation lowers the probability of $^{39}K(n,p)^{39}Ar$ to occur due to the smaller cross-section for lower energy neutrons.

These data agree with long term observations at the Berkeley Geochronology Center; in practice this has led to either completely avoiding extrapolating *J*-values determined from, e.g., outer ring standards to inner ring samples (compare Figure 3) or case to case assessment of the effects and mitigation by e.g. bracketing. The following values are calculated excluding the central well as a constraint for the planar fit.

The planar fits provide a gradient in the form of *J*/cm; to allow comparison we converted it to %/cm for the respective centre of each disk (Figure 3, Table 1). In the four irradiations in CLOCIT radial gradients range 0.2–2.4 %/cm, i.e., up to ~4% across a single disk (Table1). These compare to radial gradients in the CLICIT of up to 1%/cm (Table1). Figure 3 shows an example of radial gradients observed in two disks irradiated in CLICIT and CLOCIT. While the planar fit can provide satisfactory accuracy for most applications, the highest precision can be achieved by mixing standards and unknowns in a single well given a sufficient age difference and single grain analysis to enable distinction between standards and unknowns after the irradiation.

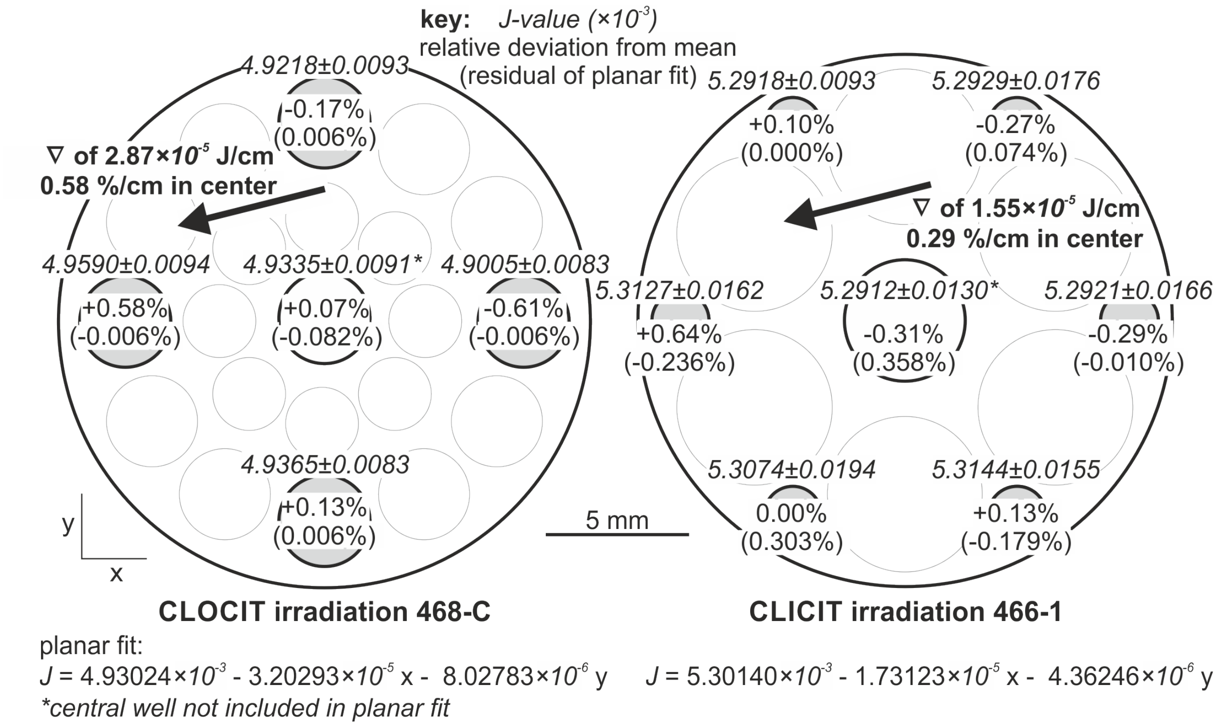

Figure 3. Maps of 21 and 13-well aluminium irradiation disks. Highlighted wells include standards. Weighted mean *J*-value, deviation from disk mean, and residual of planar fit are indicated. Arrows trace the gradient (∇); the similar orientation is coincident. Uncertainties here and throughout are given at the 1σ level. Point of origin is in the disk centres.

Interference Reactions

^{40}Ar and ^{39}Ar from K

We determined the production ratios of $(^{40}Ar/^{39}Ar)_K$ and $(^{38}Ar/^{39}Ar)_K$ which are produced via $^{39}K(n,p)^{39}Ar$, $^{40}K(n,p)^{40}Ar$, $^{39}K(n,d)^{38}Ar$, and $^{41}K(n,\alpha\beta^{-})^{38}Ar$ reactions. We analyzed CLOCIT irradiated kalsilite by single-step-fusion of 3-8 grains. 23 aliquots yielded a weighted mean of $(4\pm6)\times10^{-4}$ for $(^{40}Ar/^{39}Ar)_K$ and $(1.208\pm0.002)\times10^{-2}$ for $(^{38}Ar/^{39}Ar)_K$ (Figure 4). These values are indifferent from $(7.3\pm0.9)\times10^{-4}$ and $(1.196\pm0.013)\times10^{-2}$ for CLICIT (Renne et al., 2005). Long term repetition of this experiment is required to reduce uncertainty of the determined value for $(^{40}Ar/^{39}Ar)_K$ that is challenging to analyze precisely due to the low $^{40}Ar_K$ production rate in Cd-shielded irradiations.

^{36}Ar, ^{37}Ar, ^{38}Ar, and ^{39}Ar from Ca

We determined the production ratios of $(^{36}Ar/^{37}Ar)_{Ca}$, $(^{38}Ar/^{37}Ar)_{Ca}$ and $(^{39}Ar/^{37}Ar)_{Ca}$ which are mainly produced via $^{40}Ca(n,n\alpha)^{36}Ar$, $^{40}Ca(n,\alpha)^{37}Ar$, $^{42}Ca(n,n\alpha)^{38}Ar$, $^{43}Ca(n,n\alpha)^{39}Ar$, $^{42}Ca(n,\alpha)^{39}Ar$, and $^{43}Ca(n,n\alpha)^{39}Ar$. We analyzed fluorite irradiated in CLOCIT by single-step-fusion with a CO_2 laser. Fluorite is semitransparent to the ~10 µm wavelength of the laser so it was co-loaded with previously degassed and crushed basalt glass which co-fused the fluorite when heated. 11 aliquots of 5 to 15 grains each were analyzed. In contrast to the other isotopes, ^{39}Ar signals were only 10-30 times above background for most of the aliquots. The rise rates of the ^{39}Ar beam were significantly larger than those of the background measurements due to memory effects in the mass spectrometer. The calculated $^{39}Ar/^{37}Ar$ are overdispersed with an MSWD of 15, likely an effect of the low signal intensity and high rise rate; both effects are poorly quantified by the common uncertainty determination from intercept extrapolation. To give a more realistic representation of the uncertainty of the weighted mean of $(^{39}Ar/^{37}Ar)_{Ca}$ we multiplied the sigma uncertainty with the square-root of the MSWD and Students-t for N-1 degrees of freedom; see Ludwig (2012) for details.

The resulting weighted mean values are $(^{36}Ar/^{37}Ar)_{Ca} = (2.649\pm0.014) \times10^{-4}$, $(^{38}Ar/^{37}Ar)_{Ca} = (3.33\pm0.12) \times10^{-5}$ and $(^{39}Ar/^{37}Ar)_{Ca} = (9.1\pm0.28) \times10^{-4}$. These compare to $(^{36}Ar/^{37}Ar)_{Ca} = (2.702\pm0.004) \times10^{-4}$, $(^{38}Ar/^{37}Ar)_{Ca} = (1.96\pm0.08) \times10^{-5}$ and $(^{37}Ar/^{39}Ar)_{Ca} = (7.02\pm0.12) \times10^{-4}$ in CLICIT (Renne et al., 2015).

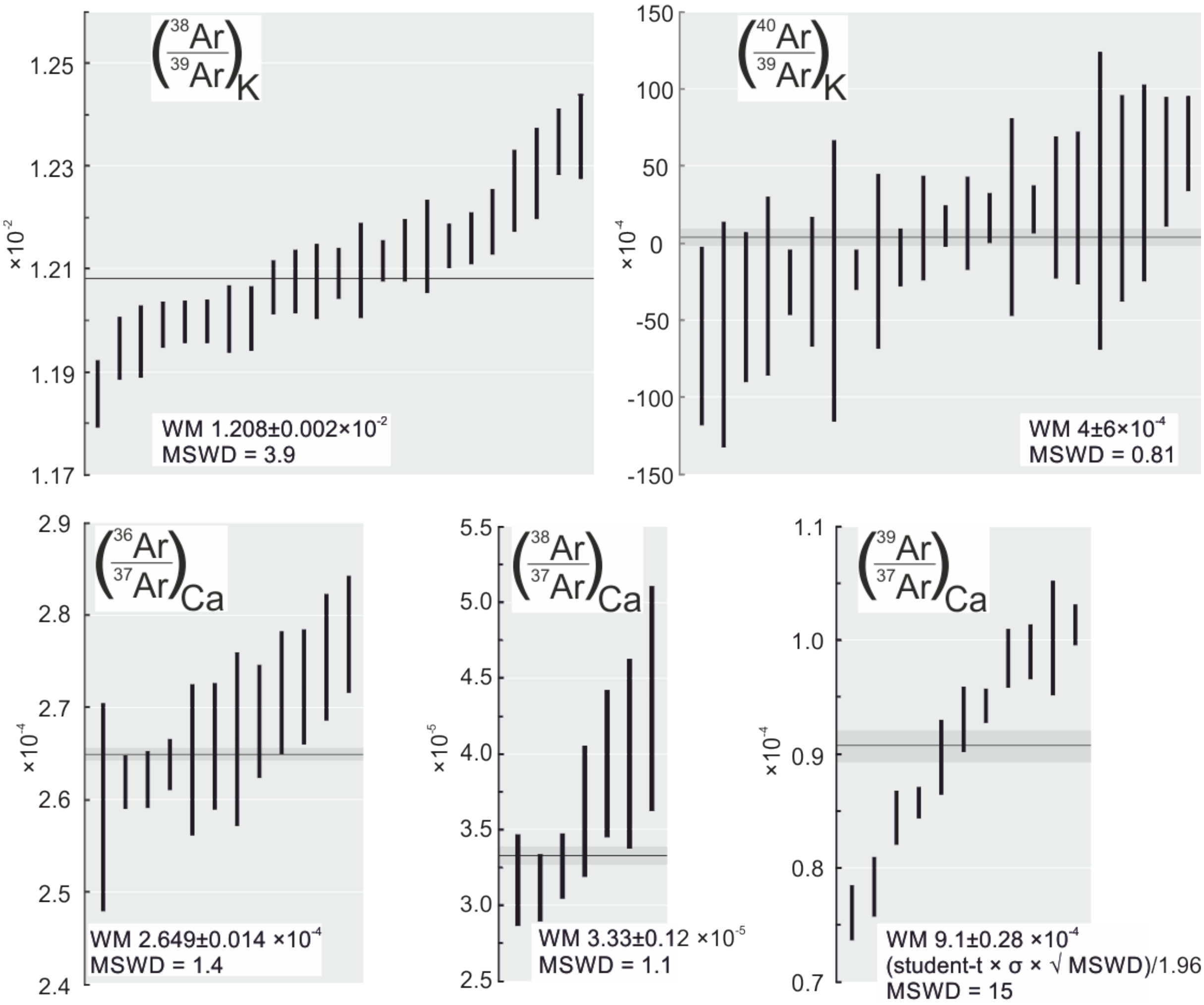

Figure 4. Ratios of Ar isotope production rates from K and Ca in CLOCIT determined from irradiated Kalsilite and Fluorite.

Conclusions

The average neutron flux is about 1.8 times lower in CLOCIT compared to CLICIT. Production rate ratios of Ar isotopes from Ca and K are similar. We find about twice as high radial fluence gradients and similar axial fluence gradients. Planar fitting of *J*-values on an irradiation disk results in residuals on the order of uncertainty in *J*, but systematic deviations can be recognized. At the current state of the technique, the non-planar component of the reactors neutron flux field becomes resolvable and needs to be accounted for to reach even higher precision and aspiring to the 0.1% goal defined by the EARTHTIME community.

Acknowledgements

D.R. was supported by DFG research scholarship RU 2065/1-1. Instrumentation was funded by NSF grants EAR-9005260, 1322017 and SBR-9601592. Facilities support from the Ann and Gordon Getty Foundation is gratefully acknowledged.

References

Grasty R. L. and Mitchell J. G. (1966) Single sample potassium-argon ages using the omegatron. *Earth Planet. Sci. Lett.* **1**, 121–122.

Kuiper K. F., Deino A., Hilgen F. J., Krijgsman W., Renne P. R. and Wijbrans J. R. (2008) Synchronizing Rock Clocks of Earth History. *Science (80-.).* **320**, 500–504. Available at: http://www.sciencemag.org/cgi/doi/10.1126/science.1154339.

Ludwig K. R. (2012) User's Manual for Isoplot 3.75. *Berkeley Geochronol. Cent. Spec. Publ.* **5**.

Niespolo E. M., Rutte D., Deino A. L. and Renne P. R. (2017) Intercalibration and age of the Alder Creek sanidine 40 Ar/ 39 Ar standard. *Quat. Geochronol.* **39**, 205–213. Available at: http://linkinghub.elsevier.com/retrieve/pii/S1871101416300589.

Renne P. R., Knight K. B., Nomade S., Leung K.-N. and Lou T.-P. (2005) Application of deuteron–deuteron (D–D) fusion neutrons to 40Ar/39Ar geochronology. *Appl. Radiat. Isot.* **62**, 25–32. Available at: http://linkinghub.elsevier.com/retrieve/pii/S0969804304003951.

Renne P. R., Sprain C. J., Richards M. A., Self S., Vanderkluysen L. and Pande K. (2015) State shift in

Deccan volcanism at the Cretaceous-Paleogene boundary, possibly induced by impact. *Science (80-.).* **350**, 76 LP-78.

Rutte D., Pfänder J. A., Koleška M., Jonckheere R. and Unterricker S. (2015) Radial fast-neutron fluence gradients during rotating 40 Ar/ 39 Ar sample irradiation recorded with metallic fluence monitors and geological age standards. *Geochemistry, Geophys. Geosystems* **16**, 336–345. Available at: http://doi.wiley.com/10.1002/2014GC005611.

Schickler R. A., Marcum W. R. and Reese S. R. (2013) Comparison of HEU and LEU neutron spectra in irradiation facilities at the Oregon State TRIGA®Reactor. *Nucl. Eng. Des.* **262**, 340–349.

Schickler R. and Reese S. (2017) Installation of a Second CLICIT Irradiation Facility at the Oregon State TRIGA Reactor. In *International Group on Research Reactors Conference Proceedings*